Transactions of JASCOME Vol. 21 (Dec. 2021), Paper No. 21-211218 JASCOME

A ROBUST TOPOLOGY OPTIMISATION IN 2D ACOUSTICS FOR IMPEDANCE MATERIALS USING THE BOUNDARY ELEMENT METHOD

Jincheng QIN[1)], Hiroshi ISAKARI[2)], Toru TAKAHASHI[3)], Toshiro MATSUMOTO[4)]

1) Nagoya University (〒 464-8603 Furo-cho, Chikusa-ku, Nagoya, E-mail: qin.jincheng@g.mbox.nagoya-u.ac.jp)
2) Keio University (〒 223-8522 3-14-1, Hiyoshi, Kohoku-ku, Yokohama, E-mail: isakari@sd.keio.ac.jp)
3) Nagoya University (〒 464-8603 Furo-cho, Chikusa-ku, Nagoya, E-mail: toru.takahashi@mae.nagoya-u.ac.jp)
4) Nagoya University (〒 464-8603 Furo-cho, Chikusa-ku, Nagoya, E-mail: t.matsumoto@nuem.nagoya-u.ac.jp)

Topology optimisation is well known as a powerful tool for designing various structures. However, the optimal structure obtained by it can fail to handle uncertainties originating from its working environment. For example, an acoustic device optimised at a given frequency cannot guarantee its performance if the frequency deviates a little from the assumption. On the other hand, it is desirable to design devices insensitive to environmental perturbation. We here develop a topology optimisation to find a robust acoustic design concerning perturbation in the exciting frequency. The design target is characterised by the impedance boundary condition. We formulate an appropriate objective function and its topological sensitivity and then incorporate them into a topology optimisation method with the level-set method. The feasibility of the present method is shown in a numerical example of sound barrier designs with wide working bandwidth.

Key Words: Robust topology optimisation, Topological derivative, Boundary element method, Acoustics

1. Introduction

Recent years have witnessed growing and extensive demands for high-performance designs. The best performance of a design depends not only on its structural and material configurations but also on the working environment which makes up the system. Owing to the consideration of both aspects, topology optimisation turns out to be one of the most flexible design tools with broad applications such as truss structure[(1)], wave lens[(2)], wave cloak[(3)], and so forth. Usually, during a standard topology optimisation (which is henceforth called "deterministic" optimisation in this paper), the structure is optimised to an ideal configuration with one or multiple fixed design parameters assumed. However, even a slight perturbation in the design parameter can, in turn, lead to a drastic deterioration in performance since the optimum works in the inevitable presence of uncertainty encountered in the real world. It is, therefore, of importance to take the uncertainties into account at the design stage.

So far, several strategies have been proposed to resolve the issue. Worst-case-based topology optimisation[(4)] is one of the most efficient approaches. Its applicable range is, however, limited because balancing the result obtained for the worst case with the deterministic optimum does not provide the structure that can handle the "intermediate" uncertainties in a complicated situation. Another strategy with the surrogate model[(5)] also has a similar weakness because a small number of sampled possibilities may often be insufficient for recovering well the physical complexity. Reliability-based topology optimisation [(6)] and the Monte-Carlo method[(7)] get various possible cases involved to emulate uncertainties in accurate manners. Their expensive computation, however, keeps away the interest of application in practice. Robust topology optimisation refines the quantification of probability with the notions of expectancy and variance. It successfully models the uncertainty with fidelity at a relatively cheap cost. Such advantages make it a prevalent topic for applications in classical structural optimisations such as compli-

Received Nov. 1, 2021, Accepted Nov. 26, 2021

ance minimisation[8, 9, 10, 11].

On the other hand, little attention has been paid to wave problems. Sato et al.[12, 13] incorporated the robust topology optimisation into designs for electromagnetic wave cloaking, in which the uncertainties in the incident frequency and angle are considered. The robustness is evaluated by the derivatives of the objective function with respect to the incident frequency and angle. Evaluating the frequency derivatives requires solving the Helmholtz equation in the exterior domain with a source term. They truncate the unbounded region using the PML boundary condition and evaluate the frequency derivatives with the finite element method (FEM). Usually, such an explicit evaluation with domain integrals involved is computationally expensive and may have limited their approximation up to second order. We have, in the previous study [14], established a boundary-element-based method to efficiently compute the derivatives. Unlike the FEM-based one, our method does not involve any volume integral and thus can naturally and efficiently deal with the exterior acoustic field. We have also pointed out that, with the help of automatic differentiation, we can facilitate the arbitrary higher-order approximation of uncertainty. With these strategies, we came up with a robust topology optimisation for acoustically rigid structures and significantly broaden the working bandwidth of acoustic devices compared with the second-order cases. Soft materials such as sponges and plastics are, however, preferred rather than rigid materials because of their flexibility and cheaper costs as usual choices for building acoustic devices. Motivated by the engineering value, in this work, we extend our robust optimisation for acoustic structures with impedance boundary conditions.

2. Problem statement of the deterministic topology optimisation

In this section, we briefly show the standard topology optimisation of deterministic type as preliminaries for presenting the proposed robust topology optimisation.

We here consider the following exterior boundary value problem (BVP) in 2D:

$$\nabla^2 p(\mathbf{x}) + k^2 p(\mathbf{x}) = 0 \quad \mathbf{x} \in \Omega, \tag{1}$$

$$p(\mathbf{x}) = 0 \quad \mathbf{x} \in \Gamma_p, \tag{2}$$

$$q(\mathbf{x}) := \mathbf{n}(\mathbf{x}) \cdot \nabla p(\mathbf{x}) = 0 \quad \mathbf{x} \in \Gamma_q, \tag{3}$$

$$q(\mathbf{x}) = \frac{i\rho\omega}{z} p(\mathbf{x}) \quad \mathbf{x} \in \Gamma_z, \tag{4}$$

$$\text{Outgoing radiation condition for } p^{\mathrm{sc}}, \tag{5}$$

where p denotes the complex amplitude of the sound pressure and q is its normal flux across the boundary $\Gamma := \overline{\Gamma_p \cup \Gamma_q \cup \Gamma_z}$. As depicted in Fig. 1, in this work we specify the normal direction $\mathbf{n}$ on Γ directed from the open fluid domain Ω. $k = \omega/v$ stands for the wavenumber, where ω and v are the angular frequency and sound speed in Ω, respectively. ρ is the density of the inviscid and compressive fluid filled in Ω. z denotes the sound impedance on Γ_z of the solid filled in $\mathbb{R}^2 \setminus \overline{\Omega}$. The sound field is assumed time-harmonic with time dependence $e^{-i\omega t}$. The Sommerfeld radiation condition (5) is imposed to guarantee the solution of scattering waves $p^{\mathrm{sc}} = p - p^{\mathrm{in}}$ to be physically outgoing, where p^{in} is the incident field. Under the constraints defined by (1)–(5). We want to find a solid object in a user-specified design domain D, i.e $\mathbb{R}^2 \setminus \overline{\Omega} \subset D$, optimising the following objective function:

$$F(\omega) = \sum_{m=1}^{M} f\left(p\left(\mathbf{x}_m^{\mathrm{obs}}\right)\right) + \int_{\Gamma} g(p(\mathbf{x}), q(\mathbf{x}))\mathrm{d}\Gamma(\mathbf{x}), \tag{6}$$

where f and g are real functionals defined on some observation points $\mathbf{x}_m^{\mathrm{obs}} \in \Omega \setminus D$ for $m = 1, \cdots, M$ and the boundary Γ, respectively.

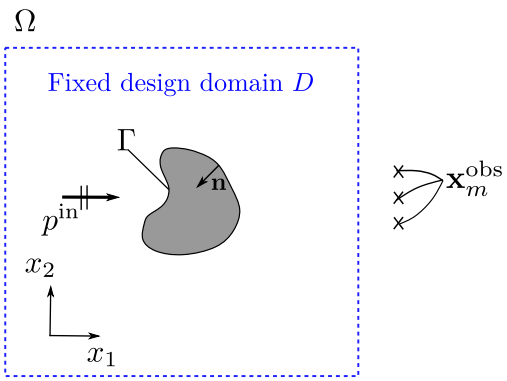

Fig. 1: Illustration of the problem.

The level-set method is employed to operate optimisations. To represent the configuration of a structure, we introduce a level-set function defined as

$$\phi(\mathbf{x}) > 0 \quad \text{if } \mathbf{x} \in \Omega \cap D, \tag{7}$$

$$\phi(\mathbf{x}) = 0 \quad \text{if } \mathbf{x} \in \Gamma, \tag{8}$$

$$\phi(\mathbf{x}) < 0 \quad \text{if } \mathbf{x} \in \mathbb{R}^2 \setminus \overline{\Omega}, \tag{9}$$

whose evolution is governed by[15]

$$\frac{\partial \phi(\mathbf{x}, t)}{\partial t} = [\mathcal{D}_{\mathrm{T}} F](\mathbf{x}, t) - (\mathcal{D}_{\mathrm{T}} F, \phi)_{L^2(D)} \phi(\mathbf{x}, t), \tag{10}$$

where

$$(\mathcal{D}_{\mathrm{T}} F, \phi)_{L^2(D)} = \int_D [\mathcal{D}_{\mathrm{T}} F](\mathbf{x}) \phi(\mathbf{x}) \mathrm{d}\Omega, \tag{11}$$

is the L^2 inner product of $\mathcal{D}_{\mathrm{T}} F$ and ϕ in the design domain D, and t is the fictitious time corresponding to an optimisation step. $\mathcal{D}_{\mathrm{T}} F$ represents the topological derivative defined as

$$[\mathcal{D}_{\mathrm{T}} F](\mathbf{x}) = \lim_{\varepsilon \downarrow 0} \frac{[\delta F]_\varepsilon(\mathbf{x})}{a(\varepsilon)}, \tag{12}$$

in which $[\delta F]_\varepsilon(\mathbf{x})$ is the change in objective functional when a circular geometric perturbation of radius ε is introduced at $\mathbf{x}$, and $a(\varepsilon)$

is a monotonically increasing function of $\varepsilon > 0$ vanishing at $\varepsilon = 0$.

We use a finite difference method to solve (10). At the beginning of every optimisation step, boundary Γ is regenerated according to the distribution of ϕ. See, for example, our previous publication[16] for more details.

When the geometric perturbation at $\mathbf{x}$ is the creation of a hole whose boundary condition is specified as the impedance boundary condition with the impedance z, the topological derivative[17] is given as

$$\left[\mathcal{D}_{\mathrm{T}} F\right](\mathbf{x}) = \Re\left[\frac{i\rho\omega p(\mathbf{x})\lambda(\mathbf{x})}{z}\right], \tag{13}$$

in a two-dimensional Helmholtz problem defined as (1)–(5), where the adjoint variable λ solving the following BVP:

$$\nabla^2\lambda(\mathbf{x}) + k^2\lambda(\mathbf{x}) + \sum_{m=1}^{M} \frac{\partial f\left(\mathbf{x}_m^{\mathrm{obs}}\right)}{\partial p}\delta\left(\mathbf{x} - \mathbf{x}_m^{\mathrm{obs}}\right) = 0 \quad \mathbf{x} \in \Omega, \tag{14}$$

$$\lambda(\mathbf{x}) = -\frac{\partial g}{\partial q}(\mathbf{x}) \quad \mathbf{x} \in \Gamma_p, \tag{15}$$

$$\mu(\mathbf{x}) := \mathbf{n}(\mathbf{x}) \cdot \nabla\lambda(\mathbf{x}) = \frac{\partial g}{\partial p}(\mathbf{x}) \quad \mathbf{x} \in \Gamma_q, \tag{16}$$

$$\mu(\mathbf{x}) = \frac{i\rho\omega}{z}\left(\lambda + \frac{\partial g}{\partial q}\right)(\mathbf{x}) + \frac{\partial g}{\partial p}(\mathbf{x}) \quad \mathbf{x} \in \Gamma_z, \tag{17}$$

$$\frac{\partial\lambda(\mathbf{x})}{\partial|\mathbf{x}|} - \mathrm{i}k\lambda(\mathbf{x}) = o\left(\frac{1}{\sqrt{|\mathbf{x}|}}\right) \quad \text{as } |\mathbf{x}| \to \infty, \tag{18}$$

is introduced. Here, δ is the Dirac delta. The forward ((1)–(5)) and adjoint BVPs (14)–(18) can be solved by using the boundary element method.

3. Robust topology optimisation

3.1. Objective function

In the aforementioned topology optimisation, the angular frequency ω describes a monochrome oscillating state. The optimal configuration evolves to fit this highly specific circumstance. As a consequence, its performance might degrade drastically when the working frequency slightly deviates from ω. If we hope to ameliorate such a sensitive behaviour of the optimum, we need to include the frequency response in the vicinity of ω in the objective function. To do this, we first introduce a stochastic variable subject to some distribution. We here assume, instead of a fixed value, that ω follows the following normal distribution:

$$\mathrm{E}[\omega] := \int_{-\infty}^{\infty} \omega \frac{e^{-\frac{(\omega-\omega_0)^2}{2\sigma^2}}}{\sqrt{2\pi}\sigma}\mathrm{d}\omega = \omega_0, \tag{19}$$

$$\mathrm{E}\left[(\omega - \omega_0)^2\right] = \sigma^2, \tag{20}$$

in which ω_0 and σ denote the expectancy and standard deviation of the (stochastic) angular frequncy, respectively. The higher-order moments[18] of the perturbation in the frequency are given as

$$\mathrm{E}\left[(\omega - \omega_0)^n\right] = s_n(n-1)!!\sigma^n, \tag{21}$$

for $n = 1, 2\cdots$ where !! represents the double factorial, and $s_n = (1 + (-1)^n)/2$ is defined. With such ω the objective function F in (6) also becomes stochastic. The expectancy $\mathrm{E}[F(\omega)]$ and variance $\mathrm{Var}[F(\omega)]$ respectively measure the average magnitude and variation of F over a frequency range of interest. With the help of Taylor series expansion, their approximation at ω can be written as

$$\mathrm{E}[F(\omega)] \simeq F(\omega_0) + \sum_{n=1}^{N} \frac{F^{(n)}(\omega_0)}{n!}\mathrm{E}\left[(\omega - \omega_0)^n\right], \tag{22}$$

and

$$\mathrm{Var}[F(\omega)] \simeq \sum_{n=1}^{N}\sum_{m=1}^{N}\left[s_{n+m}(n+m-1)!! - s_n s_m(n-1)!!(m-1)!!\right]\frac{F^{(n)}(\omega_0)}{n!}\frac{F^{(m)}(\omega_0)}{m!}\sigma^{n+m}, \tag{23}$$

respectively. For the simplicity of notation, here and in the remaining of this paper, we use $F^{(n)}$ to denote the n^{th} derivative of a variable F with respect to ω. The main idea of the robust topology optimisation is to optimise the expectancy of F meanwhile suppressing its variance. We thus define the objective function for a robust design as

$$J = (1-\eta)F(\omega_0) + \eta\left\{\sum_{n=1}^{N}\sum_{m=1}^{N}\left[s_{n+m}(n+m-1) - s_n s_m(n-1)!!(m-1)!!\right]\frac{F^{(n)}(\omega_0)}{n!}\frac{F^{(m)}(\omega_0)}{m!}\sigma^{n+m}\right\}^{\frac{1}{2}}, \tag{24}$$

in which the weight between two terms is adjusted with a coefficient $0 \le \eta \le 1$. We just keep the 0^{th} order term for the approximation of expectancy. In such a way letting $\eta = 0$ or $N < 2$ in (24) recovers the sheer deterministic objective function in (6). The standard deviation is employed instead of the variance to guarantee that the dimensions of the first and second terms in RHS of in (24) are identical to each other.

3.2. Topological derivative

The last subsection gives the objective function for the robust optimisation. By the chain rule, we can express the topological derivative corresponding to (24) as

$$\mathcal{D}_{\mathrm{T}} J = (1-\eta)[\mathcal{D}_{\mathrm{T}} F(\omega_0)] + \left\{\eta\sum_{n=1}^{N}\sum_{m=1}^{M}\left[s_{n+m}(n+m-1)!! - s_n s_m(n-1)!!(m-1)!!\right]\frac{F^{(n)}(\omega_0)}{n!}\frac{[\mathcal{D}_{\mathrm{T}} F^{(m)}](\omega_0)}{m!}\sigma^{n+m}\right\}/\sqrt{\mathrm{Var}_N\, F}, \tag{25}$$

where $\mathrm{Var}_N\, F$ denotes the RHS of (23).

We can easily compute the angular frequency derivatives of the objective functional $F^{(n)}$ in (25) by solving angular frequency differentiated boundary integral equations[14]. Also, in the previous

study, for an exterior Helmholtz problem with the Neumann boundary condition, we observe

$$\left[\mathcal{D}_{\mathrm{T}} F^{(n)}\right] = \left[\mathcal{D}_{\mathrm{T}} F\right]^{(n)}, \tag{26}$$

i.e. the differential order of an objective functional with respect to the angular frequency and a geometric change, is commutative. It is reasonable to infer that such commutativity also works for the current impedance problem. In this paper, we check (26) only numerically.

4. Numerical examples

4.1. Validation of the topological derivative

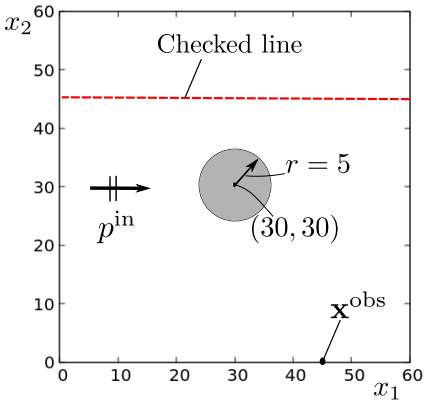

Fig. 2: Setup for the validation of the topological derivative. On the red line the topological derivative is computed.

In this section, we perform a dimensionless numerical experiment to validate the commutativity of the topological derivative (26). As depicted in Fig. 2, we put a circle of radius $r = 5$ at $(30, 30)$ whose boundary is of impedance type with $z = 3$. In the boundary element analysis, we discretised it into 200 constant elements. We specify the density of the fluid as $\rho = 1$ and the sound speed as $v = 1$. With these settings, the perpendicular sound absorption rate of the boundary is 75%. We monitor the objective function set as $F = |p(\mathbf{x}_{\mathrm{obs}})|^2$ with $\mathbf{x}_{\mathrm{obs}} = (45, 0)$ when a plane wave e^{ikx_1} with $k = 0.3$ propagates along the x_1 direction. As the topological derivatives $\mathcal{D}_{\mathrm{T}} F^{(n)}$ estimates the perturbation in the n^{th} order angular frequency derivative of the objective function $F^{(n)}$, it should coincide with the following "topological difference":

$$\left[\mathcal{D}_{T_{\mathrm{Diff}}} F^{(n)}\right](\mathbf{x}) = \frac{F_\varepsilon^{(n)}(\mathbf{x}) - F^{(n)}}{2\pi\varepsilon}, \tag{27}$$

where $F_\varepsilon^{(n)}(x) - F^{(n)}$ is the perturbation in $F^{(n)}$ when Ω_ε of radius ε is introduced at $\mathbf{x}$, if ε is sufficiently small. To check this, we computed the topological derivative as well as (27) at several points on the red line in Fig. 2. In the experiments, we used $\varepsilon = 0.0001$ for the reference. Fig. 3 and Fig. 4 shows the good agreement between the topological derivative and difference in the cases of $n = 1$ and $n = 6$, respectively. Since we have justified (26) numerically, we conclude that we may use (25) in the topology optimisation for a robust design.

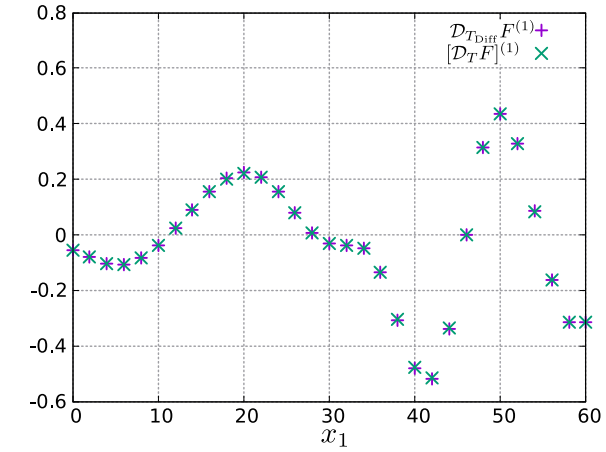

Fig. 3: Comparison between the topological difference and derivative at 1^{st} differential order

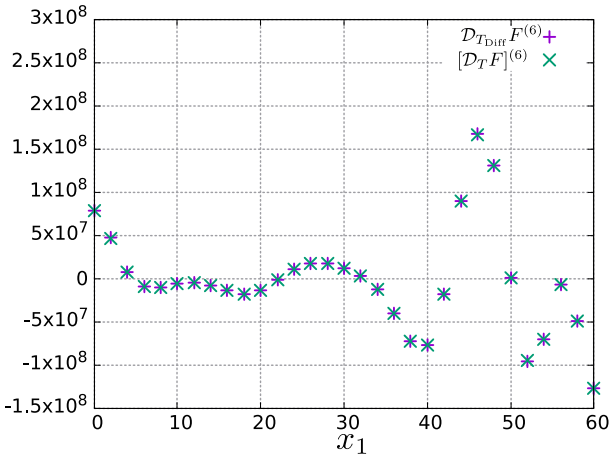

Fig. 4: Comparison between the topological difference and derivative at 6^{th} differential order

4.2. Robust design of sound barriers

This subsection presents robust designs of sound barriers using the proposed method. As depicted in Fig. 5, a circular initial configuration of radius $r = 3.2$ is put at the centre of the fixed design domain $D = [-10, 10]^2$. We explore the optimal shapes which minimises the sound norm $F = |p(\mathbf{x}_{\mathrm{obs}})|^2/2$ at $\mathbf{x}_{\mathrm{obs}} = (15, 0)$ against the incident plane wave $e^{i\omega x_1/v}$ with a mean angular frequency $\omega = 1.5$. The boundary is of impedance type with $z = 3$ prescribed. Other material constants are the same as what we used in Section 4.1. We specify $\sigma = 0.075$ and $\eta = 0\%$, 30%, and 60% for the robustness to different extents. To guarantee sufficient accuracy of approximating the frequency response[14] as $\sigma = 5\%$ of ω_0, the Taylor series expansion is truncated up to order $N = 6$. We let the unit-amplitude incident wave with the sweeping frequency $\omega \in (1, 2)$ impinge the optimal configurations shown in Fig. 6 to examine their responses. As can be seen in Fig. 7, the robust optimum can minimise the sound norm more consistently over the

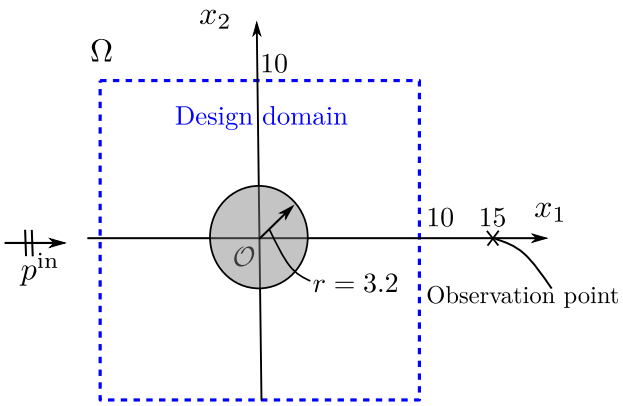

Fig. 5: Initial settings for optimisations of sound barriers

bandwidth $[\omega_0 - 3\sigma, \omega_0 + 3\sigma]$. As a contrast, at $\omega = 1.5$ the best performance of the deterministic optimum is observed. More deterministic performance is traded off for the robustness with a larger η specified. Fig. 8, Fig. 9 and Fig. 10 show the distribution of sound intensity around the optimised barriers. As can be observed in the robust designs, the size of their separate pieces has a larger variance which accounts for the handling of various incident waves with different wavelengths.

5. Conclusion

In this paper, we proposed a robust topology optimisation for structures with the impedance boundary condition. The topological derivative of a two-dimensional impedance problem has been derived and numerically validated. By using the proposed method, we successfully design sound barriers with wide working bandwidths. Our method is well suited for designing robust wave devices and can be conveniently extended for problems concerning uncertainties in other design variables such as the incident angles, the density of the fluid and so forth as long as the derivative of the objective with respective to the relevant parameter can efficiently be computed. Future related topics may also concern the acoustic-elastodynamic coupled problem for more realistic modelling of soft materials, as well as possible extensions to applications of periodic structures. Finally, it is worth mentioning that our robust topology optimisation is established based on the assumption that the frequency response of the acoustic system is smooth. In a case where the smooth condition is not satisfied, for example, if there is a real eigenvalue lying in the bandwidth of interest, the Taylor approximation can be inaccurate. It is therefore necessary to examine the distribution of eigenvalues before applying our method to either interior problems or metamaterials made up of periodic structures.

6. Acknowledgement

This study is sponsored by JSPS KAKENHI (no. 19H00740). J. Qin would like to appreciate China Scholarship Council for supporting his doctoral study.

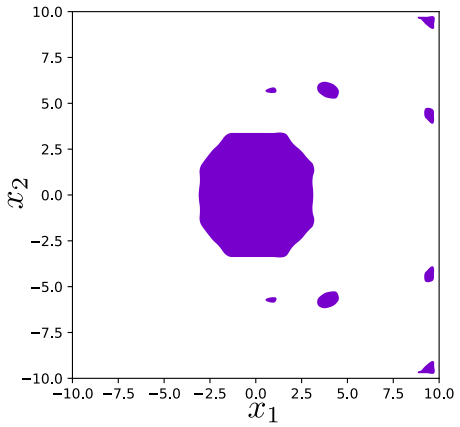

(a) $\eta = 0$ (deterministic)

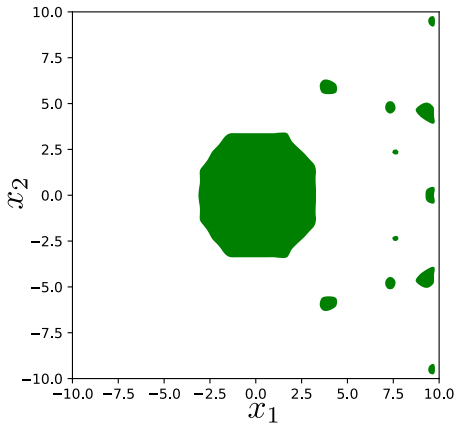

(b) $\eta = 30\%$

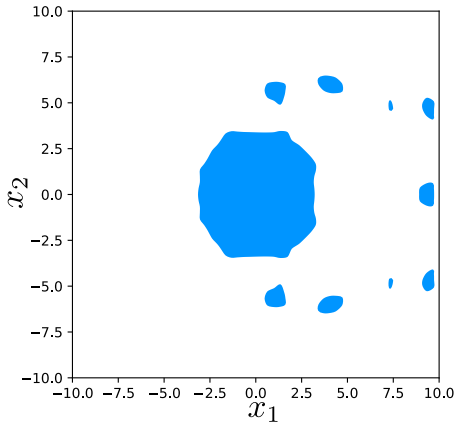

(c) $\eta = 60\%$

Fig. 6: Optimal configurations with different weight η

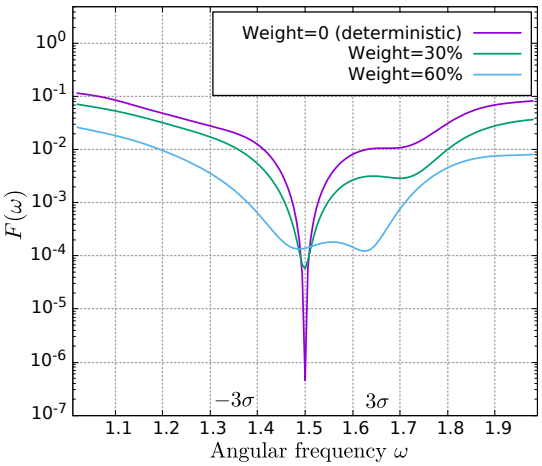

Fig.7: Frequency responses of the optimal configurations tested by the sweeping frequency

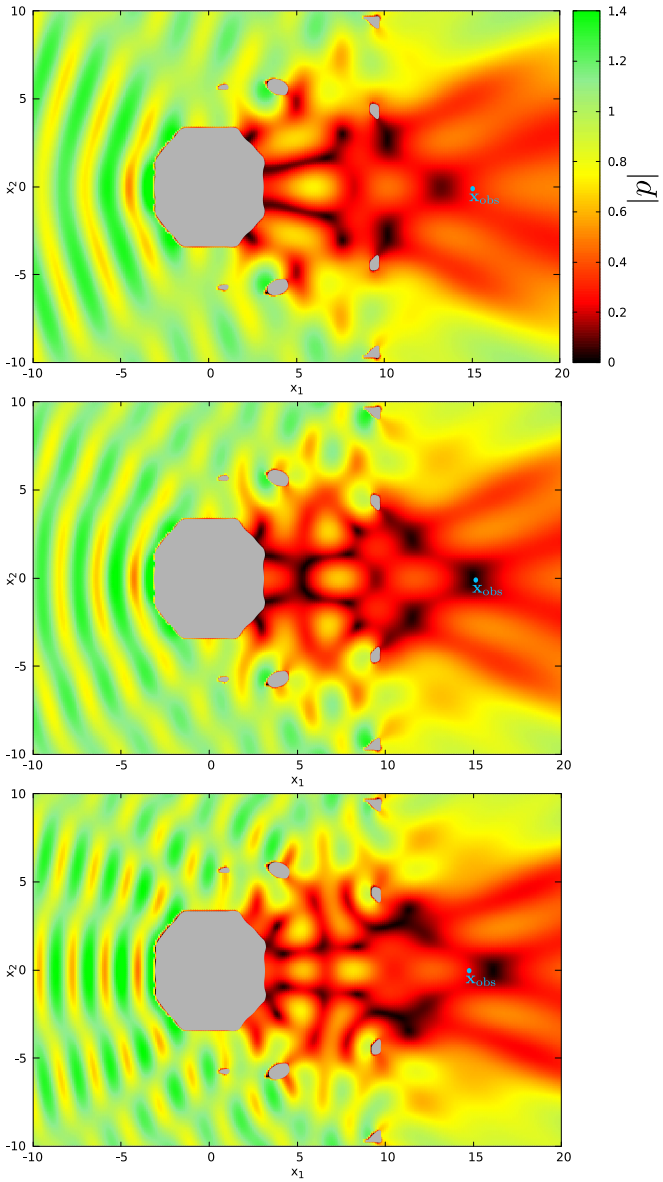

Fig. 8: Contour plots of sound intensity around the optimal sound barrier with $\eta = 0$ (deterministic) for $\omega = \omega_0 - 3\sigma$ (upper), ω_0 (middle), $\omega_0 + 3\sigma$ (lower)

参考文献

(1) Konstantinos Daniel Tsavdaridis, James J Kingman, and Vassilli V Toropov. Application of structural topology optimisation to perforated steel beams. *Computers & structures*, Vol. 158, pp. 108–123, 2015.

(2) Quang Dat Tran, Gang-Won Jang, Hyu-Sang Kwon, and Wan-Ho Cho. Shape and topology optimization of acoustic lens system using phase field method. *Structural and Multidisciplinary Optimization*, Vol. 56, No. 3, pp. 713–729, 2017.

(3) Hiroshi Isakari, Kenta Nakamoto, Tatsuya Kitabayashi, Toru Takahashi, and Toshiro Matsumoto. A multi-objective topology optimisation for 2d electro-magnetic wave problems with the level set method and bem. *European Journal of Computational Mechanics*, Vol. 25, No. 1-2, pp. 165–193, 2016.

(4) Xiaoyu Gu, John E Renaud, Stephen M Batill, Raymond M Brach, and Amarjit S Budhiraja. Worst case propagated uncertainty of multidisciplinary systems in robust design optimization. *Structural and Multidisciplinary Optimization*, Vol. 20, No. 3, pp. 190–213, 2000.

(5) Irfan Kaymaz. Application of kriging method to structural reliability problems. *Structural Safety*, Vol. 27, No. 2, pp. 133–151, 2005.

(6) Chandan Mozumder, Neal Patel, Donald Tillotson, John Renaud, and Andrés Tovar. An investigation of reliability-based topology optimization. In *11th AIAA/ISSMO Multidisciplinary Analysis and Optimization Conference*, p. 7058, 2006.

(7) Jie Liu, Guilin Wen, Qixiang Qing, Fangyi Li, and Yi Min Xie. Robust topology optimization for continuum structures with random loads. *Engineering Computations*, Vol. 35, No. 2, pp. 710–732, 2018.

(8) Nozomu Kogiso, WonJin Ahn, Shinji Nishiwaki, Kazuhiro Izui, and Masataka Yoshimura. Robust topology optimization for compliant mechanisms considering uncertainty of applied loads. *Journal of Advanced Mechanical Design, Systems, and Manufacturing*, Vol. 2, No. 1, pp. 96–107, 2008.

(9) Alireza Asadpoure, Mazdak Tootkaboni, and James K Guest. Robust topology optimization of structures with uncertainties in stiffness–application to truss structures. *Computers & Structures*, Vol. 89, No. 11-12, pp. 1131–1141, 2011.

(10) Boyan Stefanov Lazarov, Mattias Schevenels, and Ole Sigmund. Topology optimization with geometric uncertainties by perturbation techniques. *International Journal for Numerical Methods in Engineering*, Vol. 90, No. 11, pp. 1321–1336, 2012.

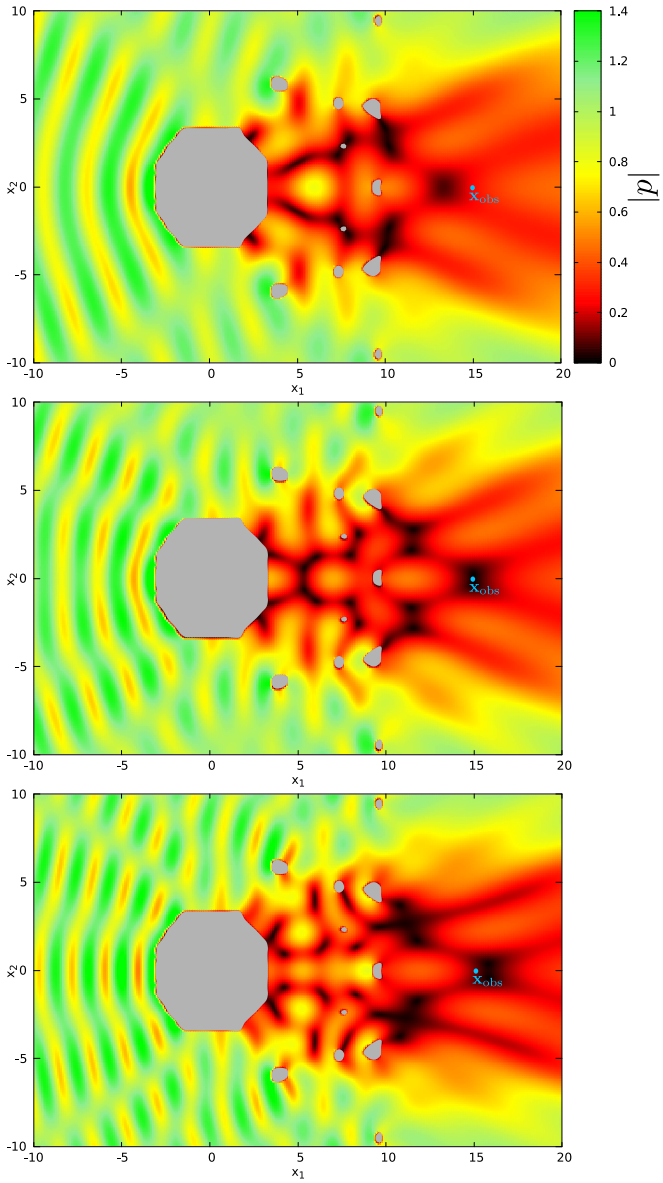

Fig. 9: Contour plots of sound intensity around the optimal sound barrier with $\eta = 30\%$ for $\omega = \omega_0 - 3\sigma$ (upper), ω_0 (middle), $\omega_0 + 3\sigma$ (lower)

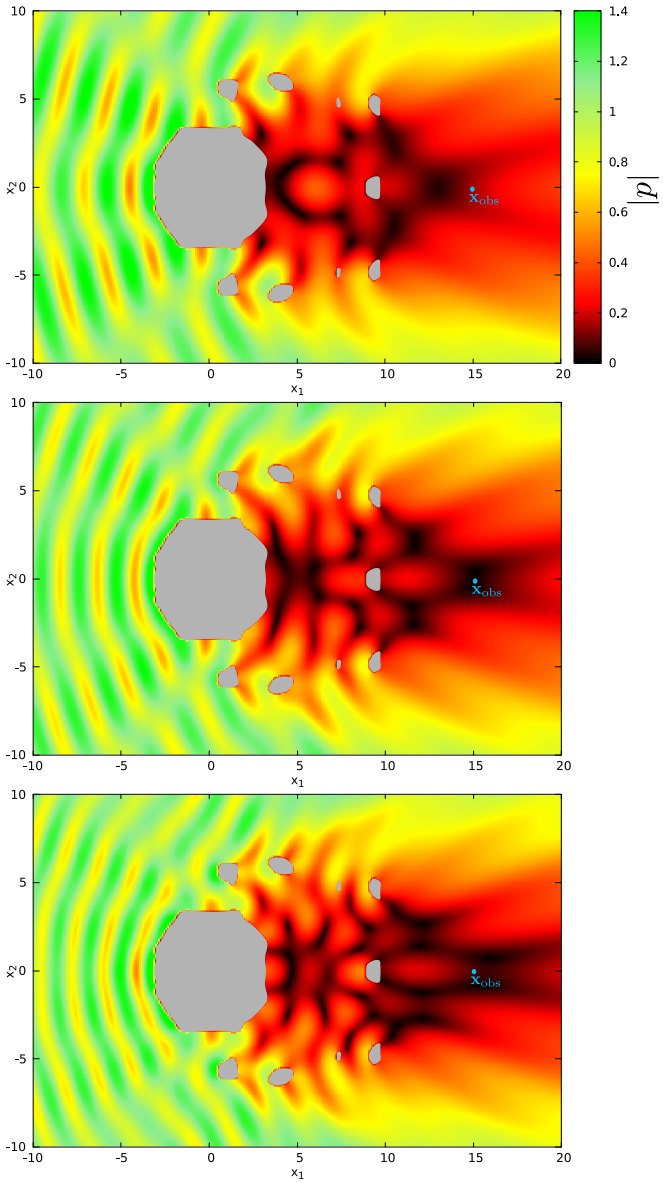

Fig. 10: Contour plots of sound intensity around the optimal sound barrier with $\eta = 60\%$ for $\omega = \omega_0 - 3\sigma$ (upper), ω_0 (middle), $\omega_0 + 3\sigma$ (lower)

(11) Qinghai Zhao, Xiaokai Chen, Zheng-Dong Ma, and Yi Lin. Robust topology optimization based on stochastic collocation methods under loading uncertainties. *Mathematical Problems in Engineering*, 2015.

(12) 佐藤勇気, 泉井一浩, 山田崇恭, 西脇眞二. 電磁クローキング構造の広帯域化を目的としたロバストトポロジー最適化. 年次大会 2017, p. J1210204. 一般社団法人 日本機械学会, 2017.

(13) Yuki Sato, Kazuhiro Izui, Takayuki Yamada, and Shinji Nishiwaki. Robust topology optimization of optical cloaks under uncertainties in wave number and angle of incident wave. *International Journal for Numerical Methods in Engineering*, Vol. 121, No. 17, pp. 3926–3954, 2020.

(14) Jincheng Qin, Hiroshi Isakari, Kouichi Taji, Toru Takahashi, and Toshiro Matsumoto. A robust topology optimization for enlarging working bandwidth of acoustic devices. *International Journal for Numerical Methods in Engineering*, Vol. 122, No. 11, pp. 2694–2711, 2021.

(15) Samuel Amstutz and Heiko Andrä. A new algorithm for topology optimization using a level-set method. *Journal of computational physics*, Vol. 216, No. 2, pp. 573–588, 2006.

(16) 飯盛浩司, 高橋徹, 松本敏郎. B スプライン曲面のレベルセットを用いたトポロジー最適化. 計算数理光学論文集, Vol. 17, pp. 125–130, 2017.

(17) 花田萌美, 飯盛浩司, 高橋徹, 松本敏郎. 2 次元音響問題における境界要素法を用いたインピーダンス境界条件を有する散乱体のトポロジー最適化. 計算数理工学論文集, Vol. 15, pp. 37–42, 2015.

(18) Harold Cramer. Mathematical methods of statistics, Princeton Univ. *Press, Princeton, NJ*, 1946.